BULLETIN OF THE POLISH ACADEMY OF SCIENCES
TECHNICAL SCIENCES, Vol. 68, No. 6, 2020
DOI: 10.24425/bpasts.2020.135388

An eddy current model of pot-cored coil for testing multilayer conductors with a hole

G. TYTKO*

Institute of Electronics, The Silesian University of Technology, ul. Akademicka 16, 44-100 Gliwice, Poland

Abstract. Pot-cored coils are commonly used as probes in eddy current testing. In this paper, an analytical model of such a coil placed over a three-layer plate with a hole has been presented. The proposed solution enables the modelling of both magnetic and non-magnetic conductive plates that contain different types of hole, i.e. a through, a surface, an inner or a subsurface hole. The problem was solved by using the truncated region eigenfunction expansion (TREE) method. The analysis was carried out in a cylindrical coordinate system in which the solution domain was radially limited. With the employment of the filamentary coil, the expressions for the magnetic vector potential, and subsequently for the impedance of the cylindrical coil were obtained. The final formulas were presented in a closed form and then implemented in Matlab. The resistance and reactance values were compared with the results obtained in the experiment and using the finite element method in the Comsol Multiphysics package. In each of the cases, good agreement was obtained.

Key words: non-destructive testing, eddy currents, coil impedance, ferrite core, truncated region eigenfunction expansion.

1. Introduction

Bringing a coil fed with alternating current closer to conductive material results in the induction of eddy currents. The presence of defects in the tested object disturbs the flow of eddy currents, which brings about changes in the impedance of the coil. The correct interpretation of these changes allows detecting flaws and estimating their geometric dimensions. What has proved to be extremely useful for this purpose are mathematical models. The employment of them makes it possible to carry out both the analysis of the obtained coil impedance components and a simulation of the measurement process. According to the author, analytical models are particularly effective, since they can be implemented in any programming language and used for calculations made directly in the measuring instrument during the test.

In a series of articles, non-destructive and semi-destructive diagnostics of concrete structures [1–3], steel elements [4, 5] and composites [6] were discussed in detail. In non-destructive testing, the inspection of materials is usually carried out with the employment of probes containing coils. The probe in the form of filamentary coil [7–10], rectangular coil [11, 12], air-cored coil [13–18], I-cored coil [19–22] and iron core coil [23] were studied. In eddy current testing, pot core probes are very frequently utilized [24, 25]. The closure of the magnetic flux inside the core makes the flux take direction towards the tested surface, which in turn causes an increase in its intensity in the near vicinity of the workpiece. The analytical model of the coil with such a core, placed over the conductive half-space was developed in [26]. However, the presented solution is insufficient because it facilitates making calculations only for objects of infinite thickness and containing an easily detectable surface hole. A comprehensive mathematical model intended for practical use in eddy current defectoscopy should allow us to model multilayer materials of finite geometric dimensions and containing a hole that may be situated anywhere in the workpiece. The novelty of this paper is an analytical solution that meets the aforementioned requirements. The developed mathematical model is designed for calculating the impedance components of an E-cored coil located above a three-layer plate with an inner hole (Fig. 1). A proper selection of workpiece parameters facilitates making calculations for both a magnetic and a non-magnetic plate containing an inner, a through, a surface or a subsurface hole.

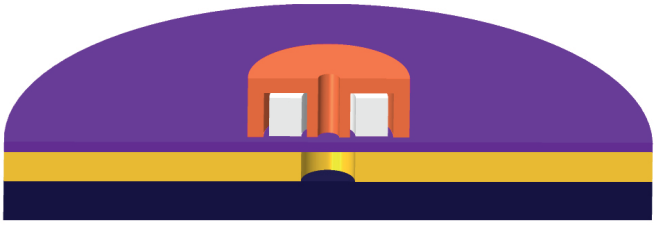

Fig. 1. E-cored coil located above a conductive plate with an inner hole

2. Methods

The cross-section of a pot-cored coil of relative magnetic permeability μ_f has been shown in Fig. 2. The coil was placed

*e-mail: grzegorz.tytko@wp.pl

Manuscript submitted 2020-05-26, revised 2020-08-11, initially accepted for publication 2020-09-11, published in December 2020

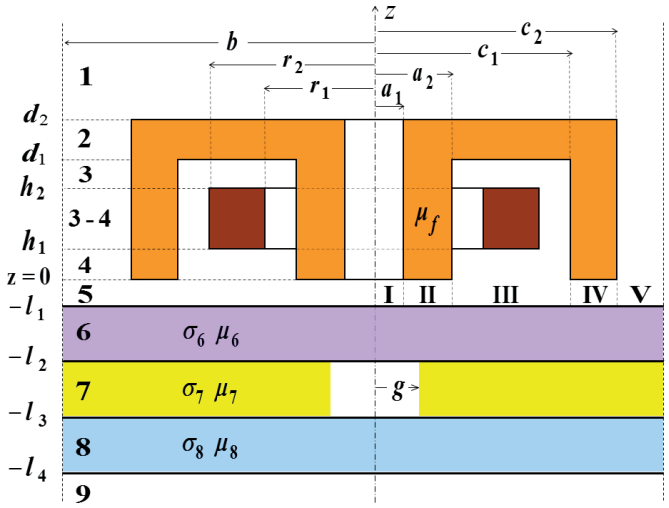

Fig. 2. Rectangular cross-sectional E-cored coil located above a three-layer conductive plate with an inner hole

at a distance l_1 from the surface of a three-layer plate of magnetic permeability of μ_6, μ_7, μ_8 and electrical conductivity σ_6, σ_7, σ_8. A hole with radius g and depth $l_3 - l_2$ was made in the middle layer of the plate. The solution domain was radially limited up to the value of parameter b. On the outer boundary $r = b$, the component of the magnetic vector potential $A_\varphi(b,z) = 0$ satisfies the Dirichlet boundary condition. While using the cylindrical coordinate system, the problem was divided into 10 regions (towards component z) and 5 subregions (I–V). For the purpose of the analysis, a filamentary coil ($r_2 - r_1 \to 0$, $h_2 - h_1 \to 0$) was employed, whose all turns coiled in a circle of radius r_0 were located at the distance h_0 from the surface of the plate. The expressions concerning the magnetic vector potential $A_\varphi(r,z)$ around such a coil were derived for each region with the employment of the truncated region eigenfunction expansion (TREE) method [27, 28] and expressed in the form of matrix notation. The number of the elements of vectors and matrices is determined by the parameter Ns. By denoting the row vectors with index $^{\mathrm{T}}$, and the column vectors of unknown coefficients as $\mathbf{C}_i$, $\mathbf{B}_i$, the following expressions were obtained:

$$\mathrm{A}_1(r,z) = J_1\left(\mathbf{q}^{\mathrm{T}} r\right) \mathbf{q}^{-1} e^{-\mathbf{q}z} \mathbf{C}_1\,, \tag{1}$$

$$\mathrm{A}_2(r,z) = \begin{matrix} \{J_1(\mathbf{m}^{\mathrm{T}} r)\} & 0 \le r \le a_1 \\ \{L_1(\mathbf{m}^{\mathrm{T}} r)\}\,\mathbf{m}^{-1}(e^{-\mathbf{m}z}\mathbf{C}_2 - e^{\mathbf{m}z}\mathbf{B}_2) & a_1 \le r \le c_2, \\ \{L_1'(\mathbf{m}^{\mathrm{T}} r)\} & c_2 \le r \le b \end{matrix} \tag{2}$$

$$\mathrm{A}_3(r,z) = \begin{matrix} \{J_1(\mathbf{p}^{\mathrm{T}} r)\} & 0 \le r \le a_1 \\ \{R_1(\mathbf{p}^{\mathrm{T}} r)\} & a_1 \le r \le a_2 \\ \{R_1'(\mathbf{p}^{\mathrm{T}} r)\}\,\mathbf{p}^{-1}(e^{-\mathbf{p}z}\mathbf{C}_3 - e^{\mathbf{p}z}\mathbf{B}_3) & a_2 \le r \le c_1, \\ \{R_1''(\mathbf{p}^{\mathrm{T}} r)\} & c_1 \le r \le c_2 \\ \{R_1'''(\mathbf{p}^{\mathrm{T}} r)\} & c_2 \le r \le b \end{matrix} \tag{3}$$

$$\mathrm{A}_4(r,z) = \begin{matrix} \{J_1(\mathbf{p}^{\mathrm{T}} r)\} & 0 \le r \le a_1 \\ \{R_1(\mathbf{p}^{\mathrm{T}} r)\} & a_1 \le r \le a_2 \\ \{R_1'(\mathbf{p}^{\mathrm{T}} r)\}\,\mathbf{p}^{-1}(e^{-\mathbf{p}z}\mathbf{C}_4 - e^{\mathbf{p}z}\mathbf{B}_4) & a_2 \le r \le c_1, \\ \{R_1''(\mathbf{p}^{\mathrm{T}} r)\} & c_1 \le r \le c_2 \\ \{R_1'''(\mathbf{p}^{\mathrm{T}} r)\} & c_2 \le r \le b \end{matrix} \tag{4}$$

$$\mathrm{A}_5(r,z) = J_1(\mathbf{q}^{\mathrm{T}} r)\mathbf{q}^{-1}(e^{-\mathbf{q}z}\mathbf{C}_5 - e^{\mathbf{q}z}\mathbf{B}_5), \tag{5}$$

$$\mathrm{A}_6(r,z) = J_1(\mathbf{q}^{\mathrm{T}} r)\mathbf{s}_6^{-1}(e^{-\mathbf{s}_6 z}\mathbf{C}_6 - e^{\mathbf{s}_6 z}\mathbf{B}_6), \tag{6}$$

$$\mathrm{A}_7(r,z) = \begin{matrix} \{J_1(\mathbf{u}^{\mathrm{T}} r)R_1(\mathbf{v}g)\} & 0 \le r \le g \\ \{R_1(\mathbf{v}^{\mathrm{T}} r)J_1(\mathbf{u}g)\} & g \le r \le b \end{matrix} \mathbf{u}^{-1}(e^{-\mathbf{u}z}\mathbf{C}_7 - e^{\mathbf{u}z}\mathbf{B}_7), \tag{7}$$

$$\mathrm{A}_8(r,z) = J_1(\mathbf{q}^{\mathrm{T}} r)\mathbf{s}_8^{-1}(e^{-\mathbf{s}_8 z}\mathbf{C}_8 - e^{\mathbf{s}_8 z}\mathbf{B}_8), \tag{8}$$

$$\mathrm{A}_9(r,z) = -J_1(\mathbf{q}^{\mathrm{T}} r)\mathbf{q}^{-1} e^{\mathbf{q}z}\mathbf{B}_9\,. \tag{9}$$

The discrete eigenvalues were written in the form of diagonal matrices **q, m, p, s**$_n$, **u, v**. For the purpose of calculating them, the employment of boundary conditions and continuity conditions of the magnetic vector potential for neighbouring subregions is the most convenient. In regions consisting exclusively of air (1, 5, 9), subregions do not exist. The discrete eigenvalues q_i of these regions are the positive real roots of the equation $J_1(q_i b) = 0$, where $J_1(x)$ is the Bessel function of the first kind. Subregions do not occur also in the upper and lower layers of the plate (6, 8). The eigenvalues s_{6i}, s_{8i} of these regions may be calculated from the expression $\mathbf{s}_n = (\mathbf{q}^2 + j\omega\mu_n\mu_0\sigma_n)^{1/2}$. In the case of region 3, discrete eigenvalues m_i were determined through solving the equation $L_1'(m_i b) = 0$, which had been formulated using the Bessel $J_n(x)$, $Y_n(x)$ function:

$$L_1'(m_i r) = \frac{\pi}{2} m_i c_2 \left[B_{2\mathrm{F}}' J_1(m_i r) + C_{2\mathrm{F}}' Y_1(m_i r)\right], \tag{10}$$

$$C_{2\mathrm{F}}' = \frac{1}{\mu_{\mathrm{f}}} J_1(m_i c_2) L_0(m_i c_2) - J_0(m_i c_2) L_1(m_i c_2), \tag{11}$$

$$B_{2\mathrm{F}}' = -\frac{1}{\mu_{\mathrm{f}}} Y_1(m_i c_2) L_0(m_i c_2) + Y_0(m_i c_2) L_1(m_i c_2), \tag{12}$$

$$L_n(m_i r) = \frac{\pi}{2} m_i a_1 \left[B_{2\mathrm{F}} J_n(m_i r) + C_{2\mathrm{F}} Y_n(m_i r)\right], \tag{13}$$

$$C_{2\mathrm{F}} = (\mu_{\mathrm{f}} - 1) J_0(m_i a_1) J_1(m_i a_1), \tag{14}$$

$$B_{2\mathrm{F}} = J_1(m_i a_1) Y_0(m_i a_1) - \mu_{\mathrm{f}} J_0(m_i a_1) Y_1(m_i a_1). \tag{15}$$

Regions 3 and 4 consist of 5 subregions each. The eigenvalues of these regions were marked as p_i and calculated from the equation:

$$R_1'''(p_i b) = 0 \tag{16}$$

where

$$R_n'''(p_i r) = \frac{\pi}{2} p_i c_2 \left[B_{3\mathrm{F}}''' J_n(p_i r) + C_{3\mathrm{F}}''' Y_n(p_i r)\right], \tag{17}$$

$$C_{3\mathrm{F}}''' = \frac{1}{\mu_{\mathrm{f}}} J_1(p_i c_2) R_0''(p_i c_2) - J_0(p_i c_2) R_1''(p_i c_2), \tag{18}$$

$$B'''_{3F} = -\frac{1}{\mu_f} Y_1(p_i c_2) R''_0(p_i c_2) + Y_0(p_i c_2) R''_1(p_i c_2), \quad (19)$$

$$R''_n(p_i r) = \frac{\pi}{2} p_i c_1 \left[B''_{3F} J_n(p_i r) + C''_{3F} Y_n(p_i r) \right], \quad (20)$$

$$C''_{3F} = \mu_f J_1(p_i c_1) R'_0(p_i c_1) - J_0(p_i c_1) R'_1(p_i c_1), \quad (21)$$

$$B''_{3F} = -\mu_f Y_1(p_i c_1) R'_0(p_i c_1) + Y_0(p_i c_1) R'_1(p_i c_1), \quad (22)$$

$$R'_n(p_i r) = \frac{\pi}{2} p_i a_2 B'_{3F} J_n(p_i r) + C'_{3F} Y_n(p_i r), \quad (23)$$

$$C'_{3F} = \frac{1}{\mu_f} J_1(p_i a_2) R_0(p_i a_2) - J_0(p_i a_2) R_1(p_i a_2), \quad (24)$$

$$B'_{3F} = -\frac{1}{\mu_f} Y_1(p_i a_2) R_0(p_i a_2) + Y_0(p_i a_2) R_1(p_i a_2), \quad (25)$$

$$R_n(p_i r) = \frac{\pi}{2} p_i a_1 \left[B_{3F} J_n(p_i r) + C_{3F} Y_n(p_i r) \right], \quad (26)$$

$$C_{3F} = (\mu_f - 1) J_0(p_i a_1) J_1(p_i a_1), \quad (27)$$

$$B_{3F} = \mu_f J_0(p_i a_1) Y_1(p_i a_1) - J_1(p_i a_1) Y_0(p_i a_1). \quad (28)$$

The presence of the hole in the conductive material results in the fact that the discrete eigenvalues u_i of region 7, and the values $v_i = (u_i^2 - j\omega\mu_7\mu_0\sigma_7)^{1/2}$ are complex numbers. In order to calculate them, it is necessary to solve (29). For this purpose, one of the methods for finding complex roots of a complex function [29-33], which are based on the Cauchy argument principle, may be used:

$$u_i \left[Y_1(v_i b) J_1(v_i g) - J_1(v_i b) Y_1(v_i g) \right] J_0(u_i g) = \\ = \frac{1}{\mu_7} v_i J_1(u_i g) \left[Y_1(v_i b) J_0(v_i g) - J_1(v_i b) Y_0(v_i g) \right]. \quad (29)$$

After all discrete eigenvalues had been determined, a system of 16 interface equations was created for the neighbouring regions. Solving this system made it possible to obtain the unknown coefficients $\mathbf{C}_i$, $\mathbf{B}_i$ which appear in expressions (1)–(9). Subsequently, these values were normalized to $\mathbf{B}_9$ and written down in the form of $\mathbf{B}_{x9} = \mathbf{B}_x/\mathbf{B}_9$ and $\mathbf{C}_{x9} = \mathbf{C}_x/\mathbf{B}_9$.

$$\begin{matrix} \mathbf{B}_{29} \\ \mathbf{C}_{29} \end{matrix} = e^{\mp \mathbf{m} d_1} \mathbf{F}^{-1} \left[(\mathbf{H} \pm \mathbf{G}) e^{\mathbf{p} d_1} \mathbf{B}_{49} + (\mathbf{H} \mp \mathbf{G}) e^{-\mathbf{p} d_1} \mathbf{C}_{49} \right], \quad (30)$$

$$\begin{matrix} \mathbf{B}_{49} \\ \mathbf{C}_{49} \end{matrix} = \mathbf{D}^{-1} \left[(\mathbf{H}' \pm \mathbf{G}') \mathbf{B}_{59} + (\mathbf{H}' \mp \mathbf{G}') \mathbf{C}_{59} \right], \quad (31)$$

$$\begin{matrix} \mathbf{B}_{59} \\ \mathbf{C}_{59} \end{matrix} = e^{\pm \mathbf{q} l_1} \left[\left(\frac{1}{\mu_6} \pm \mathbf{q} \mathbf{s}_6^{-1} \right) e^{-\mathbf{s}_6 l_1} \mathbf{B}_{69} + \right. \\ \left. + \left(\frac{1}{\mu_6} \mp \mathbf{q} \mathbf{s}_6^{-1} \right) e^{\mathbf{s}_6 l_1} \mathbf{C}_{69} \right], \quad (32)$$

$$\begin{matrix} \mathbf{B}_{69} \\ \mathbf{C}_{69} \end{matrix} = \mp e^{\pm \mathbf{s}_6 l_2} \left[- \left(\mathbf{s}_6 \mathbf{u}^{-1} \mathbf{K} \pm \mu_6 \mathbf{V} \right) e^{-\mathbf{u} l_2} \mathbf{B}_{79} + \right. \\ \left. + \left(\mathbf{s}_6 \mathbf{u}^{-1} \mathbf{K} \mp \mu_6 \mathbf{V} \right) e^{\mathbf{u} l_2} \mathbf{C}_{79} \right], \quad (33)$$

$$\begin{matrix} \mathbf{B}_{79} \\ \mathbf{C}_{79} \end{matrix} = \mp e^{\pm \mathbf{u} l_3} \left[- \left(\mathbf{s}_8^{-1} \mathbf{u} \mathbf{K}^{-1} \pm \frac{\mathbf{V}^{-1}}{\mu_8} \right) e^{-\mathbf{s}_8 l_3} \mathbf{B}_{89} + \right. \\ \left. + \left(\mathbf{s}_8^{-1} \mathbf{u} \mathbf{K}^{-1} \mp \frac{\mathbf{V}^{-1}}{\mu_8} \right) e^{\mathbf{s}_8 l_3} \mathbf{C}_{89} \right], \quad (34)$$

$$\begin{matrix} \mathbf{B}_{89} \\ \mathbf{C}_{89} \end{matrix} = e^{\pm \mathbf{s}_8 l_4} \left(\pm \mathbf{s}_8 \mathbf{q}^{-1} + \mu_8 \right), \quad (35)$$

where exponentials are diagonal matrices, $\mathbf{q}$, $\mathbf{u}$, $\mathbf{s}_6$, $\mathbf{s}_8$ are vectors and the matrices $\mathbf{F}$, $\mathbf{H}$, $\mathbf{G}$, $\mathbf{D}$, $\mathbf{H}'$, $\mathbf{G}'$, $\mathbf{K}$, $\mathbf{V}$ are defined in the Appendix.

The calculation of the coefficients $\mathbf{C}_i$, $\mathbf{B}_i$ enables determining the magnetic vector potential for each region of the system shown in Fig. 2 [34]. Through integrating over the cross section of the coil, the expression describing the potential of region 3–4, the formula for the impedance of the E-cored coil placed over the three-layer plate with the inner hole was derived:

$$Z = \frac{j\omega\pi\mu_0 N^2}{[(r_2 - r_1)(h_2 - h_1)]^2} \chi(\mathbf{p}^{\mathrm{T}}) \mathbf{p}^{-1} \left\{ \left[e^{-\mathbf{p}h_2} e^{\mathbf{p}h_1} - e^{\mathbf{p}h_2} e^{-\mathbf{p}h_1} + \right. \right. \\ \left. + 2\mathbf{p}(h_2 - h_1) \right] + \left[- \left(e^{\mathbf{p}h_2} - e^{\mathbf{p}h_1} \right) \mathbf{B}_{49} + \left(e^{-\mathbf{p}h_1} - e^{-\mathbf{p}h_2} \right) \mathbf{C}_{49} \right] \cdot \\ \cdot \left(-\mathbf{B}_{29} + \frac{\mathbf{T} - \mathbf{U}}{\mathbf{T} + \mathbf{U}} e^{-2\mathbf{m}d_2} \mathbf{C}_{29} \right)^{-1} \left(\boldsymbol{\lambda}_1 - \frac{\mathbf{T} - \mathbf{U}}{\mathbf{T} + \mathbf{U}} e^{-2\mathbf{m}d_2} \boldsymbol{\lambda}_2 \right) \Bigg\} \cdot \\ \mathbf{D}^{-1} \chi(\mathbf{p}), \quad (36)$$

where

$$\chi(\mathbf{x}) = \int_{\mathbf{x}r_1}^{\mathbf{x}r_2} r R'_1(\mathbf{x}r) \, \mathrm{d}r, \quad (37)$$

$$\begin{matrix} \boldsymbol{\lambda}_1 \\ \boldsymbol{\lambda}_2 \end{matrix} = \mathbf{F}^{-1} \left[(\mathbf{H} \mp \mathbf{G}) e^{-\mathbf{p}d_1} \left(e^{\mathbf{p}h_2} - e^{\mathbf{p}h_1} \right) + \right. \\ \left. + (\mathbf{H} \pm \mathbf{G}) e^{\mathbf{p}d_1} \left(e^{-\mathbf{p}h_1} - e^{-\mathbf{p}h_2} \right) \right] e^{\mp \mathbf{m}d_1}, \quad (38)$$

$$\mathbf{T} = [t_{ij}] = [\mu_f a_1 J_1(q_i a_1) J_0(m_j a_1) - c_2 J_1(q_i c_2) L_0(m_j c_2)] \\ \frac{q_i}{q_i^2 - m_j^2} \left(\frac{1}{\mu_f} - 1 \right), \quad (39)$$

$$\mathbf{U} = [u_{ij}] = [a_1 J_0(q_i a_1) J_1(m_j a_1) - c_2 J_0(q_i c_2) L_1(m_j c_2)] \\ \frac{q_i}{q_i^2 - m_j^2} \left(\frac{1}{\mu_f} - 1 \right). \quad (40)$$

The obtained expression makes it possible to calculate the coil impedance components for various configurations. An appropriate selection of the parameters of the modelled system allows taking into consideration the following cases:

- the absence of a conductor ($\sigma_6 = \sigma_7 = \sigma_8 = 0$),
- a plate without a hole ($g = 0$),
- a plate with a surface hole ($\sigma_6 = 0$),
- a plate with a through-hole ($\sigma_6 = \sigma_8 = 0$),
- a plate with an air gap between the layers ($\sigma_7 = 0$),
- a plate with a subsurface hole ($\sigma_8 = 0$),
- an air-cored coil ($\mu_f = 1$).

3. Results and discussions

In order to determine the component values of the coil impedance, (36) was implemented in Matlab. The eigenvalues m_i and p_i were calculated with the employment of the fzero( ) procedure, whereas u_i – with the MCCE method [35]. The integral (37) was calculated by using the expansion of the Bessel and Struve functions [28]. The geometric dimensions of individual elements of the system, and parameter values used in the calculations have been presented in Table 1. The obtained results were verified experimentally and with the employment of the finite element method (FEM) in the COMSOL Multiphysics package. The mesh used in the numerical model contained: 28774 triangular elements, 14576 mesh vertices, 1171 edge elements and 30 vertex elements. The highest density of mesh elements was used around the hole and under the coil. The time necessary to calculate components of the coil impedance was about 3.5 seconds for the TREE method and 9 seconds for the FEM method, using a computer with an Intel Core i5 processor equipped with the 6 GB RAM. For the needs of the research, a measurement system consisting of the Agilent E4980A precision LCR meter, an eddy current probe, material samples and a PC computer was built. The measurements of the electrical conductivity of materials were carried out with the employment of the Foerster Sigmatest 2.069 device. The upper layer of the tested object was a brass plate of the conductivity of $\sigma_6 = 14.3\,\mathrm{MSm}^{-1}$, which was placed on the plates of the thickness of $l_4 - l_2 = 15$ mm made of aluminium ($\sigma_7 = \sigma_8 = 20.5\ \mathrm{MSm}^{-1}$) or copper ($\sigma_7 = \sigma_8 = 58.9\ \mathrm{MSm}^{-1}$). In these plates a hole of the diameter of $2g = 2.75$ mm and the depth of $l_3 - l_2 = 10.3$ mm (aluminium) and $l_3 - l_2 = 10.1$ mm (copper) was made. What was accepted as the final results was the arithmetic mean determined for 3 measurement series.

Table 1
Parameters of the coil, core and plate used in calculations

Number of turns	N	646
Inner column radius	a_1	1.5 mm
Outer column radius	a_2	3.9 mm
Inner core radius	c_1	7.6 mm
Outer core radius	c_2	9 mm
Inner core height	d_1	4.2 mm
Outer core height	d_2	5.3 mm
Inner coil radius	r_1	4.4 mm
Outer coil radius	r_2	7.5 mm
Offset	h_1	0.2 mm
Parameter	h_2	4.1 mm
Radius of the hole	g	1.375 mm
Liftoff	l_1	0.2 mm
Parameter	l_2	0.48 mm
Parameter	l_4	15.48 mm
Conductivity	σ_6	14.3 MSm^{-1}
Relative permeability	μ_6, μ_7, μ_8	1
Relative permeability	μ_f	3000
Radius of the domain	b	$20\,r_2$
Summation terms	Ns	90

The values of the changes of the coil impedance components $\Delta Z = R - R_0 + j\omega(X - X_0)$ after bringing it closer to the plate with an inner hole, were normalized with respect to the coil reactance in the air space X_0, and shown in Figs. 3 and 4. The calculations and measurements were made for 50 values of frequency in the range from 500 Hz to 20 kHz. The values of the coil impedance changes in the case of the copper and the aluminium plates for frequency $f = 1$ kHz and $f = 20$ kHz have been shown in Table 2. The maximum values of the error concerning δ_R resistance and δ_X reactance in the TREE and

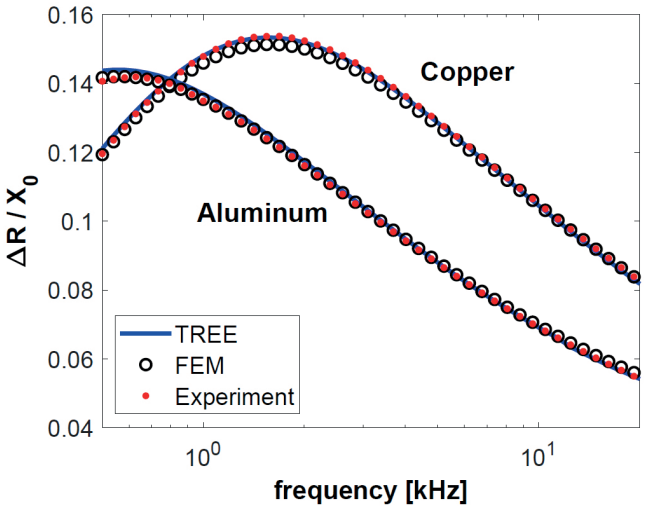

Fig. 3. Changes of the coil resistance normalized with respect to X_0 for frequencies from 500 Hz to 20 kHz

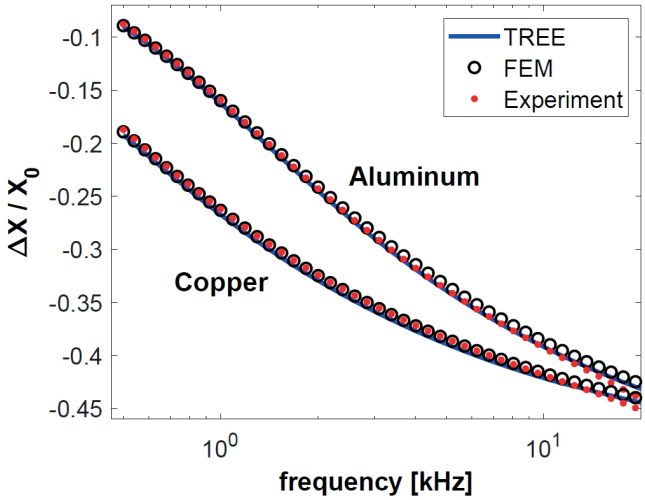

Fig. 4. Changes of the coil reactance normalized with respect to X_0 for frequencies from 500 Hz to 20 kHz

Table 2
Values of the changes in coil impedance $\Delta Z = \Delta R + j\Delta X$

Material	f [kHz]	Experiment	TREE	FEM
Aluminium	1	$17.08 - j18.40\Omega$	$17.10 - j18.74\Omega$	$16.85 - j18.46\Omega$
	20	$191.3 - j1022.3\Omega$	$189.4 - j1000.7\Omega$	$191.3 - j989.7\Omega$
Copper	1	$15.58 - j30.27\Omega$	$15.82 - j30.87\Omega$	$15.64 - j30.40\Omega$
	20	$125.4 - j1046.9\Omega$	$125.4 - j1030.5\Omega$	$128.1 - j1022.6\Omega$

FEM methods obtained in the tested frequency range have been shown in Table 3.

Table 3
The highest values of the errors δ_R and δ_X of coil impedance components

Material	TREE		FEM	
	δ_R [%]	δ_X [%]	δ_R [%]	δ_X [%]
Aluminium	1.25	2.91	1.62	3.18
Copper	2.17	2.60	2.11	2.33

$$\delta_R = \left| \frac{R_{measure} - R_{calculate}}{R_{measure}} \right| \cdot 100\%, \tag{41}$$

$$\delta_X = \left| \frac{X_{measure} - X_{calculate}}{X_{measure}} \right| \cdot 100\%. \tag{42}$$

4. Conclusion

The developed mathematical model facilitates calculating the components of the impedance of an E-cored coil located above the surface of a three-layer plate with a hole. The employment of the proposed solution enables modelling both magnetic and non-magnetic materials containing a hole located in any layer of the tested element. In this way it is possible to examine materials of any thickness, i.e. from thin foils to thick plates. What is an unquestionable merit of the analytical model are the final formulas presented in a closed form, thanks to which they may be implemented in any programming language as well as in mathematical packages, such as Mathematica and Matlab. By replacing time-consuming integrals by the series, a short time of calculations was obtained. The correct selection of the number of summation terms Ns and the constraints of the solution domain g make it possible to effectively control the calculation error and to determine the size of the matrices, so as to avoid excessive iterations. The verification of the results carried out with the help of the experiment and finite element methods pointed to good agreement. In the case of the changes of resistance and the changes of reactance, the error did not exceed 2.17% and 2.91%, respectively.

Appendix

The matrices **F**, **H**, **G**, **D**, **H′**, **G′**, **K**, **V** were written in the following form:

$$\mathbf{F} = [f_i] = \frac{1}{2}\left(\frac{1}{\mu_f} - 1\right)\left\{a_1^2\left[\mu_f J_0^2(m_i a_1) - J_1^2(m_i a_1)\right] + \right.$$
$$\left. + c_2^2\left[L_1^2(m_i c_2) - \frac{1}{\mu_f} L_0^2(m_i c_2)\right]\right\} + \frac{b^2}{2} L_0'^2(m_i b), \tag{43}$$

$$\mathbf{H} = [h_{ij}] = \left[a_2 L_0(m_i a_2) R_1(p_j a_2) + \right.$$
$$\left. - c_1 L_0(m_i c_1) R_1'(p_j c_1)\right] \frac{m_i}{m_i^2 - p_j^2}\left(1 - \frac{1}{\mu_f}\right), \tag{44}$$

$$\mathbf{G} = [g_{ij}] = \left[\frac{1}{\mu_f} a_2 L_1(m_i a_2) R_0(p_j a_2) + \right.$$
$$\left. - c_1 L_1(m_i c_1) R_0'(p_j c_1)\right] \frac{m_i}{m_i^2 - p_j^2}\left(1 - \frac{1}{\mu_f}\right), \tag{45}$$

$$\mathbf{D} = [d_i] = \frac{1}{2}\left\{a_1^2\left[J_0^2(p_i a_1) + J_1^2(p_i a_1) - \frac{1}{\mu_f}\Phi(p_i a_1)\right] + \right.$$
$$- a_2^2\left[\Phi'(p_i a_2) - \frac{1}{\mu_f}\Phi(p_i a_2)\right] + c_1^2\left[\Phi'(p_i c_1) + \right.$$
$$\left. - \frac{1}{\mu_f}\Phi''(p_i c_1)\right] - c_2^2\left[\Phi'''(p_i c_2) - \frac{1}{\mu_f}\Phi''(p_i c_2)\right]$$
$$\left. + b^2\Phi'''(p_i b)\right\}, \tag{46}$$

$$\mathbf{H'} = [h_{ij}'] = \left[\mu_f a_1 J_0(p_i a_1) J_1(q_j a_1) - a_2 R_0(p_i a_2) J_1(q_j a_2) + \right.$$
$$\left. + \mu_f c_1 R_0'(p_i c_1) J_1(q_j c_1) - c_2 R_0''(p_i c_2) J_1(q_j c_2)\right] \cdot$$
$$\cdot \frac{p_i}{p_i^2 - q_j^2}\left(1 - \frac{1}{\mu_f}\right), \tag{47}$$

$$\mathbf{G'} = [g_{ij}'] = \left[a_1 J_1(p_i a_1) J_0(q_j a_1) - a_2 R_1(p_i a_2) J_0(q_j a_2) + \right.$$
$$\left. + c_1 R_1'(p_i c_1) J_0(q_j c_1) - c_2 R_1''(p_i c_2) J_0(q_j c_2)\right] \cdot$$
$$\cdot \frac{p_i}{p_i^2 - q_j^2}\left(1 - \frac{1}{\mu_f}\right), \tag{48}$$

$$\mathbf{K} = [k_{ij}] = \boldsymbol{\beta}_1 + \boldsymbol{\beta}_2, \tag{49}$$

$$\mathbf{V} = [v_{ij}] = \boldsymbol{\beta}_1 + \frac{1}{\mu_7}\boldsymbol{\beta}_2 , \tag{50}$$

$$\boldsymbol{\beta}_1 = R_1(v_j g)\left[q_i J_0(q_i g) J_1(u_j g) - \right. \\ \left. - u_j J_1(q_i g) J_0(u_j g)\right] \frac{g}{u_j^2 - q_i^2} , \tag{51}$$

$$\boldsymbol{\beta}_2 = -J_1(u_j g)\left[q_i J_0(q_i g) R_1(v_j g) - \right. \\ \left. - v_j J_1(q_i g) R_0(v_j g)\right] \frac{g}{v_j^2 - q_i^2} . \tag{52}$$

References

[1] C. Maierhofer, G. Zacher, C. Kohl, and J. Wöstmann, "Evaluation of Radar and Complementary Echo Methods for NDT of Concrete Elements", *J. Nondestruct. Eval.* 27, 47–57 (2008).

[2] A. Garbacz, "Application of stress based NDT methods for concrete repair bond quality control", *Bull. Pol. Ac.: Tech.* 63 (1), 77–85 (2015).

[3] J. Hoła, J. Bień, Ł. Sadowski, and K. Schabowicz, "Nondestructive and semi-destructive diagnostics of concrete structures in assessment of their durability", *Bull. Pol. Ac.: Tech.* 63 (1), 87–96 (2015).

[4] I. Altpeter, G. Dobmann, and K. Szielasko, "Electromagnetic NDT to characterize usage properties of flat steel products", *CINDE Journal* 36 (4), 6–9 (2015).

[5] R. Kędra and M. Rucka, "Preload monitoring in a bolted joint using Lamb wave energy", *Bull. Pol. Ac.: Tech.* 67 (6), 1161–1169 (2019).

[6] C.F. John *et al.*, "Corrosion behavior of ZrC particles reinforcement with Al-12Si composites by weight loss method using acidic media", *Bull. Pol. Ac.: Tech.* 66 (1), 9–16 (2018).

[7] I. Babic, F. Sirois, and C. Akyel, "Validity check of mutual inductance formulas for circular filaments with lateral and angular misalignments", *Prog. Electromagn. Res. M* 8, 15–26 (2009).

[8] S. Zhang, J. Tang, and W. Wu, "Comparison the impedance calculation models of coil above conductive plates", in *IEEE International Conference on Mechatronics and Automation (ICMA)*, Beijing, China, 2015.

[9] L. Liang, "Analysis of inductance calculation of coaxial circular filamentary coils, thin-wall solenoids, and disk coils using inverse hyperbolic functions", *IET Sci. Meas. Technol.* 10, 754–760 (2016).

[10] G. Tytko and L. Dziczkowski, "Fast calculation of the filamentary coil impedance using the truncated region eigenfunction expansion method", *ACES Journal*, 33, 1461–1466 (2018).

[11] Y. Zhilichev, "Analysis of eddy currents in rectangular coils by integral equation method in sub-domains", *IEEE Trans. Magn.* 50, 7028110 (2014).

[12] S. Zhang, J. Tang, and W. Wu, "Calculation model for the induced voltage of pick-up coil excited by rectangular coil above conductive plate", *2015 IEEE International Conference on Mechatronics and Automation (ICMA)*, Beijing, 2015, pp. 1805–1810, doi: 10.1109/ICMA.2015.7237760.

[13] P. Putek *et al.*, "Two-level approach for solving the inverse problem of defects identification in Eddy Current Testing – type NDT", *Arch. Electr. Eng.* 60, 497–518 (2011).

[14] V. Chudacik and M. Smetana, "Tilt-shift eddy current probe impact on information value of response signal", *Arch. Electr. Eng.* 65, 133–140 (2016).

[15] D. Wen, M. Fan, B. Cao, Z. Xue and P. Wang, "A PEC thrice subtraction method for obtaining permeability invariance feature in conductivity measurement of ferromagnetic samples", *Appl. Sci.* 9, 2745 (2019).

[16] Z. Xue, M. Fan, B. Cao, and D. Wen, "A fast numerical method for the analytical model of pulsed eddy current for pipelines", *Insight – Non-Destructive Testing and Condition Monitoring* 62, 27–33 (2020).

[17] O. Martens *et al.*, "Fast precise eddy current measurement of metals", *IEEE International Instrumentation and Measurement Technology Conference (I2MTC)*, Houston, USA, 2018.

[18] F. Jiang and S. Liu, "Calculation and analysis of an analytical model for magnetic field monitoring based on TREE in eddy current testing", *ACES Journal* 33, 1489–1497 (2018).

[19] Y. Le Bihan, J. Pávó, and C. Marchand, "Characterization of small cracks in eddy current testing", *IET Colloquium on Reliability of Electromagnetic Systems*, Paris, France, 2007.

[20] Y. Lu, J.R. Bowler, and T.P. Theodoulidis, "An analytical model of a ferrite-cored inductor used as an eddy current probe", *J. Appl. Phys.* 111, 103907 (2012).

[21] G. Tytko and L. Dziczkowski, "I-cored coil probe located above a conductive plate with a surface hole", *Meas. Sci. Rev.* 18, 7–12 (2018).

[22] Y. Zhu, B. Chen, Y. Luo, and R. Zhu, "Inductance calculations for coaxial iron-core coils shielded by cylindrical screens of high permeability", *IET Electr. Power Appl.* 13 (6), 802–811 (2019), doi: 10.1049/iet-epa.2018.5667.

[23] Ł. Majka, "Applying a fractional coil modelfor power system ferroresonance analysis", *Bull. Pol. Ac.: Tech.* 66 (4), 367–474 (2018).

[24] T.L. Cung, P.Y. Joubert, E. Vourch, and P. Larzabal, "Interactions of an eddy current sensor and a multilayered structure", *Electronics Letters* 46, 1550–1551 (2010).

[25] F. Sakkaki and H. Bayani, "Solution to the problem of E-cored coil above a layered half-space using the method of truncated region eigenfunction expansion", *J. Appl. Phys.* 111, 07E717 (2012).

[26] G. Tytko and L. Dziczkowski, "Calculation of the impedance of an E-cored coil placed above a conductive material with a surface hole", *Meas. Sci. Rev.* 19, 43–47 (2019).

[27] T.P. Theodoulidis and J.R. Bowler, "The truncated region eigenfunction expansion method for the solution of boundary value problems in eddy current non-destructive evaluation", *Rev. Prog. Quant. Nondestruct. Eval.* 24A, 403–408 (2004).

[28] T.P. Theodoulidis and E.E. Kriezis, *Eddy Current Canonical Problems (With Applications to Nondestructive Evaluation)*. Tech Science Press, Duluth (Georgia), USA, 2006.

[29] D. Vasic, D. Ambru, V. Bilas, "Computation of the eigenvalues for bounded domain eddy-current models with coupled regions", *IEEE Trans. Magn.* 52, 7004310 (2016).

[30] T. Theodoulidis and A. Skarlatos, "Computation of eigenvalues and eigenfunctions in the solution of eddy current problems with modal methods", *22nd International Conference on the Computation of Electromagnetic Fields (COMPUMAG 2019)*, Paris, France, 2019.

[31] L. Delves and J. Lyness, "A numerical method for locating the zeros of an analytic function", *Math. Comput.* 21, 543–560 (1967).

[32] M. Dellnitz, O. Schutze, and Q. Zheng, "Locating all the zeros of an analytic function in one complex variable", *J. Comput. Appl. Math.* 138, 325–333 (2002).

[33] P. Kravanja, M. Barel, O. Ragos, M.N. Vrahatis, and F.A. Zafiropoulos, "ZEAL: A mathematical software package for computing zeros of analytic functions", *Comput. Phys. Commun.* 124, 212–232 (2000).

[34] C.V. Dodd and W.E. Deeds, "Analytical solutions to eddy-current probe-coil problems", *J. Appl. Phys.* 39, 2829–2838 (1968).

[35] G. Tytko and Ł. Dawidowski, "Locating complex eigenvalues for analytical eddy-current models used to detect flaws", *Compel-Int. J. Comp. Math. Electr. Electron. Eng*. 38, 1800–1809 (2019).